ELSEVIER

Brain Research 927 (2002) 55–68

BRAIN RESEARCH

www.elsevier.com/locate/bres

Research report

A *Shaker* homologue encodes an A-type current in *Xenopus laevis*

Hubert H. Kerschbaum[a,*], Stephan Grissmer[b], Edwin Engel[c], Klaus Richter[d], Christine Lehner[a], Heike Jäger[b]

[a]*Department of Molecular Neurobiology and Cellular Physiology, Institute of Zoology, University of Salzburg, Hellbrunnerstr. 34, 5020 Salzburg, Austria*

[b]*Department of Applied Physiology, University Ulm, Albert Einstein Allee 11, 89081 Ulm, Germany*

[c]*Austrian Academy of Sciences, Institute of Molecular Biology, Billrothstraße 11, 5020 Salzburg, Austria*

[d]*Institute of Genetics, University of Salzburg, Hellbrunnerstr. 34, 5020 Salzburg, Austria*

Accepted 22 November 2001

Abstract

In *Xenopus laevis*, several distinct K^+-channels (xKv1.1, xKv1.2, xKv2,1, xKv2.2, xKv3.1) have been cloned, sequenced, and electrophysiologically characterized. K^+-channels significantly shape neuronal excitability by setting the membrane potential, and latency and duration of action potentials. We identified a further *Shaker* homologue, xKv1.4, in *X. laevis*. The open reading frame encodes a K^+-channel that shares 72% of its 698 amino acids with the human *Shaker* homologue, hKv1.4. Northern blot analysis revealed xKv1.4 in the brain, muscle, and spleen but not in the ovary, intestine, heart, liver, kidney, lung, and skin. Whole-cell patch clamp recording from rat basophilic leukaemia (RBL) cells transfected with xKv1.4 revealed a voltage-gated, outward rectifying, transient A-type, K^+ selective current. xKv1.4 was strongly dependent on extracellular K^+. Exposure of cells to K^+ free bath solution almost completely abolished the current, whereas in the presence of high K^+, inactivation in response to a maintained depolarizing step and the frequency-dependent cumulative inactivation decreased. Ion channels encoded by xKv1.4 are sensitive to 4-aminopyridine and quinidine but insensitive to tetraethylammonium and the peptide toxins, charybdotoxin, margatoxin, and dendrotoxin. In conclusion, our results indicate that the biophysical and pharmacological signature of xKv1.4 closely resemble those of the A-current described in *Xenopus* embryonic neurons and is similar to the human *Shaker* homologue, hKv1.4.

Theme: Excitable membranes and synaptic transmission

Topic: Potassium channel structure, function, and expression

Keywords: Potassium channel; Kv1.4; Neuron; *Xenopus*

1. Introduction

Several types of ion channels, including voltage-gated K^+-channels, have been characterized in neurons of *Xenopus laevis*. Cloning, sequencing, and heterologous expression provided evidence for several distinct voltage-gated K^+-channels in *X. laevis* (xKv1.1, xKv1.2, xKv2.1, xKv2.2, and xKv3.1), which differ in their voltage sensitivity, their kinetic property, and their sensitivity to different pharmacological agents [5,14,24,30,33,34]. In addition, electrophysiological evidence exists for a rapidly activating and inactivating current, generally known as A-current, in *Xenopus* primary spinal neurons and muscle fibers [12,30]. In *Xenopus* embryonic neurons, activation of an A-current correlates with shortening of action potentials and development of phasic firing in response to a maintained depolarization [28]. In mammals, several genes encoding K^+-channels with an A-like current have been characterized [6]. However, the molecular structure of the K^+-channel responsible for the A-current in *X. laevis* is not known.

This paper describes the identification of an ion channel encoded by a *Shaker* homologue in *X. laevis*. This gene encodes a channel characterized by rapid activation and inactivation. The deduced amino acid sequence of this K^+-channel shares 72% similarity with the human *Shaker*

*Corresponding author. Tel.: +43-662-8044-5667; fax: +43-662-8044-5698.

E-mail address: hubert.kerschbaum@sbg.ac.at (H.H. Kerschbaum).

0006-8993/02/$ – see front matter
PII: S0006-8993(01)03324-8

homologue, hKv1.4. Furthermore, the biophysical properties and the pharmacological sensitivity to different agents were indistinguishable from mammalian Kv1.4. Therefore, we named the *Shaker* homologue in *Xenopus*, xKv1.4. Our results indicate that the channel encoded by xKv1.4 is a candidate for the A-current in embryonic neurons of *X. laevis*.

2. Material and methods

2.1. Identification of a Shaker homologue

A λZAPII complementary DNA (cDNA) library, prepared from *X. laevis* brain mRNA (Stratagene, La Jolla, CA, USA), was screened under medium stringency conditions (300 mM NaCl, 2 mM EDTA, 20 mM Sodium phosphate, pH 8, 60 °C) with a ^{32}P-labelled fragment of rat Kv1.3. Strongly hybridising phages were isolated and subcloned into pBluescript SK^+ (Stratagene UV Stratalinker 2400, USA). cDNA inserts were sequenced according to the dideoxy chain termination method [32].

The complete coding sequence of xKv1.4 was amplified by PCR and subcloned into the pBluescriptSK^+ vector. The following primers were used: 5′ GAGAGAATTCATGGAGGTTGCCATGGTG 3′ (EcoRI primer, EcoRI site underlined) and 5′ GAGACTCGAGTCACACATCAGTTTCCAGAATTTT 3′ (XhoI primer, XhoI site is underlined). The coding sequence was then transcribed according to the in vitro transcription kit T7 Cap-Scribe (Boehringer Mannheim, Germany).

2.2. RNA isolation and Northern blot analysis

Total RNA was extracted from brain, heart, muscle, spleen, kidney, lung, liver, intestine, ovary, and skin of *X. laevis* using the guanidinium thiocyanate–phenol–chloroform method [7] with minor modifications. In brief, organs were homogenized in 4.2 M guanidinium thiocyanate and 1% β-mercaptoethanol. Nucleic acids were extracted in phenol–chloroform and RNA was isolated by acid extraction and isopropanol precipitation.

Total RNA (10 μg) were denatured by heating for 5 min at 65 °C and electrophoresed on 1.2% formaldehyde–agarose gels, transferred onto nylon membranes (0.45 μm, Boehringer Mannheim, Germany), and UV crosslinked in the stratalinker (Stratagene UV Stratalinker 2400, USA). After prehybridization for 150 min in a solution of Church buffer (1% bovine serum albumin, 1 mM EDTA, 0.5 M Na^+-phosphate, 7% sodium dodecyl sulphate) and 100 μg/ml denatured herring sperm DNA at 60 °C, hybridization with a radioactive-labeled DNA probe was performed overnight at 60 °C. Random primed labeling was done according to the instructions from Boehringer Mannheim. Following hybridization, membranes were washed twice in a solution consisting of 0.2× standard saline phosphate EDTA (SSPE) and 0.1% sodium-dodecyl-sulfate at 60 °C. Blots were exposed to Kodak X Omat UV film at −70 °C with intensifying screen for 1 week.

2.3. Cell culture and electrophysiology

Rat basophilic leukaemia (RBL-2H3) cells were maintained in Eagle's minimal essential medium (EMEM) supplemented with 1 mM L-glutamine and 10% heat-inactivated foetal calf serum, in a humified 5% CO_2 incubator at 37 °C.

RNA was transcribed from cDNA and injected into RBL cells. RBL cells are electrophysiologically well characterized and do not express detectable voltage-gated outward rectifying K^+-channels [21]. The cRNA was diluted with 0.5% fluorescein-5-isothiocyanate (FITC) Dextran MW 10 000 in 100 mM KCl to a final concentration of 0.5–1 mg/ml. The cRNA/FITC-solution was filled into injection capillaries (Femtotips, Eppendorf, Germany) and RBL cells were injected using an Eppendorf microinjection system (Micromanipulator 5171 and Transjector 5246) as described [18,23,27]. Two to six hours later, injected cells were identified by fluorescence and whole-cell currents were investigated.

Patch clamp recordings were performed in the whole cell mode on cRNA injected RBL cells [15] as described earlier [19,23,27]. Microelectrodes were pulled from glass capillaries (Clark Electromedical Instruments, Reading, UK), coated with Sylgard (Dow Corning Corp., Midland, MI), and fire polished to resistances of 2–5 MΩ. All experiments were done at room temperature (21–25 °C). The bath solution contained (in mM): 160 NaCl, 4.5 KCl, 2 $CaCl_2$, 1 $MgCl_2$, 10 Hepes, titrated to pH 7.4 with NaOH (290–320 mosmol l^{-1}) or 160 KCl, 2 $CaCl_2$, 1 $MgCl_2$, 10 Hepes, titrated to pH 7.4 with KOH (290–320 mosmol l^{-1}). In some experiments, 160 mM KCl was substituted by equimolar concentrations of RbCl, CsCl, NaCl, or NH_4Cl. The pipette solution contained (in mM): 134 KF, 1 $CaCl_2$, 2 $MgCl_2$, 10 Hepes, 10 EGTA, titrated to pH 7.2 with KOH (290–320 mosmol l^{-1}). External solutions were changed by a syringe-driven perfusion system. Peptide toxin block was measured in the presence of 0.1% bovine serum albumin. CTX, MgTX and DTX were purchased from Alamone (Jerusalem, Israel). All other chemicals were from Sigma (St Louis, MO). Membrane currents were recorded with an EPC-9 patch clamp amplifier (HEKA elektronik, Lambrecht, Germany), filtered at 2.9 kHz, and digitized. Stimulation and recording was controlled by a Macintosh computer with appropriate software (Pulse and PulseFit). Series resistance compensation (80%) was used, if the current exceeded >2 nA. All figures were corrected for capacitative and leak currents using templates created by averaging and scaling 10 current traces elicited during hyperpolarizing voltage

pulses (P/10 procedure). Peak conductance was calculated using the equation

$$g_K = I_K/V - E_K$$

where g_K is the K^+ conductance of the peak current amplitude, I_K is the maximum K^+ current during each depolarizing voltage step, V is the membrane potential, and E_K is the reversal potential of K^+ as calculated according to the Nernst equation. E_K was assumed to be -86 mV. Data points were fitted to a Boltzmann distribution

$$g_{K_v} = g_{K_{max}}/[1 + e^{((V_n - V)/k)}]$$

where g_{K_v} is the conductance at a given potential, $g_{K_{max}}$ the maximum conductance, V_n the voltage at the midpoint of the curve, and k is the slope factor.

3. Results

3.1. Identification and expression of xKv1.4 in the X. laevis nervous system

We used a cDNA library from *X. laevis* brain to screen for *Shaker* genes expressed in *Xenopus* nervous system, using a cDNA encoding Kv1.3 as a probe. We have identified a transcript that shows sequence similarities with known voltage-gated K^+-channels. Sequencing the full-length cDNA clone revealed an open reading frame of 2094 nucleotides encoding a 698 amino acid protein (Fig. 1). The predicted amino acid sequence revealed six transmembrane domains (S1–S6), a GYGD motif, which is characteristic for K^+ selective ion channels [6], and phosphorylation sites for protein kinase C, protein kinase A, and tyrosine kinase. Fig. 1 shows a diagram of the cDNA structure and the deduced amino-acid sequence of a *Shaker* channel in *X. laevis*. The predicted amino acid sequence displays 72% similarity with the human Kv1.4 (hKv1.4) (Fig. 2). Therefore, we consider it as the *Xenopus* homologue of mammalian Kv1.4 and named it xKv1.4. Recently, Fry et al. reported the sequence of xKv1.4 expressed in the muscle of *X. laevis* [13]. xKv1.4 expressed in brain and muscle, respectively, share 95% similarity in their primary sequence (Table 1). To avoid confusion, we will refer to xKv1.4 expressed in the muscle tissue as xKv1.4m. Mammalian Kv1.4 (hKv1.4, rKv1.4, mKv1.4) and xKv1.4 differ mainly in their N-terminal portion. The similarity of the initial 174 amino acids between xKv1.4 and hKv1.4 is 31%. The main reasons for this difference are missing amino acid sequences in the N-terminal region and amino acid sequences in the segments between transmembrane domain one and two and three and four, which are not present in mammalian Kv1.4. Domains of high homology include the pore region, the six putative transmembrane domains, and the C terminal region.

Northern blot analysis was used to investigate the tissue-specific expression of xKv1.4 in adult *X. laevis*. Brain, muscle, and spleen expressed xKv1.4 whereas skin, ovary, intestine, liver, kidney, lung, and heart did not show a detectable signal (Fig. 3).

3.2. Biophysical and pharmacological properties of xKv1.4

Whole cell voltage-clamp recording from RBL cells expressing homooligomers of xKv1.4 revealed rapidly activating and inactivating outward K^+-currents in response to a family of depolarizing voltage pulses (Fig. 4A). The xKv 1.4-current activated around -60 mV and reached half maximum activation at -26 ± 3 mV (mean$\pm$S.D.) ($n=5$ cells) (Fig. 4B). The amplitude of the xKv1.4 current is a function of the holding potential. The current amplitude was similar at holding potentials between -120 and -60 mV. However, at holding potentials more depolarized than -60 mV, the current decreased. Mean half inactivation was reached at -43 mV ($n=5$ cells) (Fig. 4C).

Macroscopic K^+-current was fitted with a single time constant for activation (τ_m), whereas the inactivation is a biexponential process and was fitted with a fast time constant (τ_f) and a slow time constant (τ_s). The time constant of activation (τ_m) showed a voltage-dependent decrease from a mean of 2.6 ± 0.5 ms at -50 mV to 0.4 ± 0.1 ms at $+50$ mV ($n=5$ cells) (Fig. 4D). In contrast to the time constant of activation, the time constant of inactivation was hardly voltage-dependent (Fig. 4E). At $+40$ mV, inactivation of the macroscopic current was fitted with $\tau_f = 23.7\pm0.8$ ms and $\tau_s = 118.1\pm21$ ms ($n=5$ cells).

In cells dialysed with low Ca^{2+} (10 nM), inactivation gradually decreased (Fig. 5). However, individual time constants τ_f and τ_s did not change, whereas their relative contribution to inactivation changed with time. At the beginning of recording, the slow time constant τ_s contributed 15% to inactivation. After the outward current developed a stable peak current and inactivation, τ_s contributed 37% to the inactivation while the fast inactivating component τ_f had decreased during dialysis from 85 to 63%. A similar observation has been reported by Roeper et al. [31] in mammalian Kv1.4 channels. These authors suggested that a Ca^{2+}-dependent phosphorylation–dephosphorylation process was responsible for this effect.

Reversal potential, as an indicator of K^+ selectivity, was studied using tail currents. Since deactivation of K^+-channels in 4.5 mM $[K^+]_e$ was too fast to be unequivocally visualized, we increased $[K^+]_e$ from 4.5 to 16 mM to slow down the time course of deactivation. With 16 mM extracellular K^+ and 134 mM intracellular K^+, tail currents reversed polarity between -60 and -50 mV ($n=5$ cells), which is predicted by the Nernst equation. Increasing $[K^+]_e$ further to 160 mM shifted the reversal potential

```
1 ATG GAG GTT GCC ATG GTG AGC GCG GAC AGT TCC GGC TGT AGC       42
  M   E   V   A   M   V   S   A   D   S   S   G   C   S

 43 AAC CAC CTG CCT TAC GGA TAT GCA CAG GCC CGC GCC CGC GAG       84
     N   H   L   P   Y   G   Y   A   Q   A   R   A   R   E

 85 CGG GAA CGC CAG GCG CAT TCC CGC GCC GCA GCC GCT GCC GCT      126
     R   E   R   Q   A   H   S   R   A   A   A   A   A   A

127 GCT TCT GGA GAA GGC GGG AAC TCA GGG GGC GGA GCC GGA GTG      168
     A   S   G   E   G   G   N   S   G   G   G   A   G   V

169 AAC GCG CGG CGC GCG CCT CAG AAT CAA GTG CCA GAG CAG CAA      210
     N   A   R   R   A   P   Q   N   Q   V   P   E   Q   Q

211 GAG GAG AAG TCA TCG CAG AAA AAG AAA AGT GCC AGG CGG AGG      252
     E   E   K   S   S   Q   K   K   K   S   A   R   R   R

253 TAC TGG CCA CTA AGC GGC TGC AAC AGG TGG AGG AGC CGG CAC      294
     Y   W   P   L   S   G   C   N   R   W   R   S   R   H

295 AAC GAA TGC AGC GGA GGC GCT GGA GGA AGA AGA GCA GGA GGA      336
     N   E   C   S   G   G   A   G   G   R   R   A   G   G

337 GAA GAC GAC GGC ACC TTC CCC TCG GAG CTG GGT CTA TGC GGC      378
     E   D   D   G   T   F   P   S   E   L   G   L   C   G

379 TCT GAG GAG ATG ATG CTC AGG GAA GAG GTG GCT GAG GAG GAC      420
     S   E   E   M   M   L   R   E   E   V   A   E   E   D

421 CAA AAG TTT TAC ATT TGT GAA GAG GAT GAT AAG GAG GCC AAC      462
     Q   K   F   Y   I   C   E   E   D   D   K   E   A   N

463 AGC CTG CAC AGG AGG AGA AGC CCC ACA GAG GAT GGA TAT CAC      504
     S   L   H   R   R   R   S   P   T   E   D   G   Y   H

505 CCT GTG TAC AGC GAG TTT GAG TGC TGT GAG AGG AGA AGC CCC      546
     P   V   Y   S   E   F   E   C   C   E   R   R   S   P
```

Fig. 1. cDNA and predicted protein sequence of xKv1.4.

to 0 mV ($n=5$ cells), as predicted by the Nernst equation (data not shown), indicating a K^+-channel.

K^+-channels are highly selective for K^+ over other monovalent cations [17]. The structural substrate for the K^+ selectivity is a G(Y/F)GD motif in the pore region [6]. xKv1.4 contains a GYGD motif in the pore region between position 570 and 573. We studied the selectivity of xKv1.4 by substitution of K^+ with an equivalent amount of the permeant monovalent cations Rb^+, Cs^+, Na^+, and NH_4^+ and measured the reversal potential. The reversal potential of the cations used was estimated from instantaneous I/V curves. Instantaneous I/V curves were obtained using a

```
547 ACA GAG GAT GGA TAT CAC CCT GTG TAC AGC GAG TTT GAG TGC 588
    T   E   D   G   Y   H   P   V   Y   S   E   F   E   C

589 TGT GAG AGG GTC GTG ATC AAC GTG TCA GGA ATG CGC TAT GAG 630
    C   E   R   V   V   I   N   V   S   G   M   R   Y   E

631 ACC CAG CTA AAA ACT TTG AGC CAG TTT CCC GAA ACT CTG CTG 672
    T   Q   L   K   T   L   S   Q   F   P   E   T   L   L

673 GGC GAC CCA GAA AAA AGG ACG CGC TAT TTC GAC CCT CTG AGG 714
    G   D   P   E   K   R   T   R   Y   F   D   P   L   R

715 AAC GAG TAT TTC TTC GAC CGC AAC CGC CTG AGT TTC GAC TCC 756
    N   E   Y   F   F   D   R   N   R   L   S   F   D   S

757 ATC CTA TAC TAC TAC CAG TCC GGG GGA AGG CTG AAG CGG CCG 798
    I   L   Y   Y   Y   Q   S   G   G   R   L   K   R   P

799 GTC AAC GTG CCC TTC GAC ATC TTT TCC GAG GAG GTC AAG TTT 840
    V   N   V   P   F   D   I   F   S   E   E   V   K   F

841 TAC GAA TTG GGA GAG GAG GCC TTG CTA AAA TAC CGC GAG GAT 882
    Y   E   L   G   E   E   A   L   L   K   Y   R   E   D

883 GAA GGT TTC GTT AAA GAG GAA GAA AAG CAG CTG CCA GAA AAT 924
    E   G   F   V   K   E   E   E   K   Q   L   P   E   N

925 GAG TTC AAG AAG CAA GTG TGG CTA CTG TTT GAG TAC CCG GAA 966
    E   F   K   K   Q   V   W   L   L   F   E   Y   P   E

967 AGT TCG GGG GCA GCT CGG GGC ATT GCC ATC GTC TCA GTG CTG 1008
    S   S   G   A   A   R   G   I   A   I   V   S   V   L

1009 GTC ATT CTA ATC TCC ACT GTC ATC TTT TGT TTG GAA ACA TTA 1050
     V   I   L   I   S   T   V   I   F   C   L   E   T   L

1051 CCG GAG TTC AGG GAT GAC AAG GAT AAT TTG CTG TCT CCG CTG 1092
     P   E   F   R   D   D   K   D   N   L   L   S   P   L

1093 GGA ATG GGG GAT GAT GAT GGT GCA GGG GAA GAT GGA GAG GGA 1134
     G   M   G   D   D   D   G   A   G   E   D   G   E   G
```

Fig. 1. (*continued*)

20-ms prepulse from −100 to +40 mV, followed by discrete voltage steps between −120 and +40 mV in 10-mV increments. The most permeant cation was K^+ and the least permeant cation was Na^+ with a P_X/P_K ratio of 1 and <0.01, respectively. The selectivity sequence was $K^+ \geq Rb^+ \gg NH_4^+ > Cs^+ \gg Na^+$ ($n=5$ cells). These data

```
1135 GGG GCT TAC AAT GCA ACT TTT CTA TCA ACA GAT AGT GGT CAC     1176
     G   A   Y   N   A   T   F   L   S   T   D   S   G   H

1177 ACT GCA TTT AAT GAT CCA TTT TTT ATA GTG GAG ACT GTG TGC     1218
     T   A   F   N   D   P   F   F   I   V   E   T   V   C

1219 ATT GTC TGG TTC TCC TTT GAG TTT GCT GTG CGC CTT TTT GCT     1260
     I   V   W   F   S   F   E   F   A   V   R   L   F   A

1261 TGC CCG AGC AAA CCT GAA TTT TTT AAA AAC ATA ATG AAC ATA     1302
     C   P   S   K   P   E   F   F   K   N   I   M   N   I

1303 ATA GAC ATT GTG TCC ATT TTG CCT TAC TTT ATC ACC CTG GGT     1344
     I   D   I   V   S   I   L   P   Y   F   I   T   L   G

1345 ACT GAG CTT GGG CAG CAG CAC CCC CCT CAG CAG CAG CAG CAC     1386
     T   E   L   G   Q   Q   H   P   P   Q   Q   Q   Q   H

1387 CTT GCC CTA GCT ACA GGG CAA CAA CTT CCC CAG GGA ACT GGG     1428
     L   A   L   A   T   G   Q   Q   L   P   Q   G   T   G

1429 CAG CAA CAG CAG GCT ATG TCC TTT GCT ATT CTG AGG ATA ATT     1470
     Q   Q   Q   Q   A   M   S   F   A   I   L   R   I   I

1471 CGC CTG GTT AGG GTC TTC CGA ATC TTT AAA TTG TCC AGG CAT     1512
     R   L   V   R   V   F   R   I   F   K   L   S   R   H

1513 TCC AAG GGG CTG CAG ATA CTT GGT CAC ACC TTG AGA GCC AGC     1554
     S   K   G   L   Q   I   L   G   H   T   L   R   A   S

1555 ATG AGG GAA CTG GGA TTA CTC ATC TTC TTT CTT TTC ATT GGG     1596
     M   R   E   L   G   L   L   I   F   F   L   F   I   G

1597 GTC ATT CTA TTC TCA AGT GCT GTT TAT TTT GCA GAG GCT GAT     1638
     V   I   L   F   S   S   A   V   Y   F   A   E   A   D

1639 GAA CCC ACA ACC CAC TTT CAG AGC ATC CCT GAT GCC TTC TGG     1680
     E   P   T   T   H   F   Q   S   I   P   D   A   F   W

1681 TGG GCT GTT GTT ACA ATG ACC ACA GTG GGT TAT GGG GAT ATG     1722
     W   A   V   V   T   M   T   T   V   G   Y   G   D   M
```

Fig. 1. (*continued*)

suggest that xKv1.4, like other voltage-gated K^+-channels, is highly selective for K^+.

Previous work on mammalian Kv1.4 has shown that removal of extracellular K^+ $[K^+]_e$ almost completely abolished the K^+ current, whereas increasing $[K^+]_e$ slowed inactivation and reduced frequency-dependent inactivation [6,25]. Strong dependence of mammalian Kv1.4 on $[K^+]_e$ is due to a lysine in the outer pore region [25]

```
1723 AAG CCC ATT ACT GTT GGG GGT AAG ATA GTG GGC TCC CTG TGT     1764
      K   P   I   T   V   G   G   K   I   V   G   S   L   C

1765 GCC ATA GCA GGG GTA TTG ACT ATC GCA CTA CCA GTG CCA GTG     1806
      A   I   A   G   V   L   T   I   A   L   P   V   P   V

1807 ATA GTT TCA AAC TTT AAC TAC TTT TAC CAC AGG GAA ACT GAC     1848
      I   V   S   N   F   N   Y   F   Y   H   R   E   T   D

1849 AAT GAT GAA CAA ACA CAG TTG TCA CAG AGC AGC TCC AGC TGC     1890
      N   D   E   Q   T   Q   L   S   Q   S   S   S   S   C

1891 CCA TAC TTA CCC ACC ATC CTA TTG AAA AAG TTG AGG AGC TCC     1932
      P   Y   L   P   T   I   L   L   K   K   L   R   S   S

1933 ACA TCT TCC TCT CTT CAG GAC AAG TCT GAA TAT CTA GAG ATG     1974
      T   S   S   S   L   Q   D   K   S   E   Y   L   E   M

1975 GAG GAA GGG CTC AAA GAG TCT CTC TGT GTA AAG GAC AAG GCT     2016
      E   E   G   L   K   E   S   L   C   V   K   D   K   A

2017 AGT GAG GGT ACA TGG AAT GGC AAC GAG ACC ATT AAG TAT AAC     2058
      S   E   G   T   W   N   G   N   E   T   I   K   Y   N

2059 TGT GTG AAT TTA AAA ATT CTG GAA ACT GAT GTG TGA     2094
      C   V   N   L   K   I   L   E   T   D   V   Z
```

Fig. 1. (*continued*)

and on electrostatic repulsion of the inactivation gate. Since xKv1.4 has a lysine residue at position 575 in the outer pore region and shows 72% sequence similarity with hKv1.4 on its N-terminal end (initial 25 amino acids), we assumed a strong $[K^+]_e$ dependence of the channel. Fig. 6 illustrates the effect of $[K^+]_e$ on current amplitude, inactivation, and frequency-dependent cumulative inactivation. In the absence of $[K^+]_e$, the peak current is reversibly reduced by ~90% (Fig. 6A). Elevated $[K^+]_e$ decreases the inactivation during a depolarizing pulse nearly completely. Frequency-dependent cumulative inactivation was investigated by applying 200-ms voltage pulses from −80 to +40 mV every second. The peak amplitude of the K^+ current during the second voltage step was considerably smaller in normal bath solution than in K^+ solution (160 mM K^+). On average, in normal bath solution the current was reduced to 50% ($n=3$ cells) and in K^+ solution to 85% ($n=3$ cells) (Fig. 6B,C). These data provide strong evidence that $[K^+]_e$ plays an important role in gating and kinetic of xKv1.4 channels.

Channels responsible for transient currents are encoded by different genes and show different sensitivity to pharmacological agents [6]. Patch clamp analysis of *Xenopus* embryonic spinal neurones revealed a 4-aminopyridine (4-AP) sensitive but tetraethylammonium (TEA) insensitive A-current [30]. Only ion channels encoded by the mammalian *Shaker* homologue Kv1.4 display properties reported from the *Xenopus* A-current, including rapid activation and inactivation and 4-AP sensitivity but TEA insensitivity [6]. Therefore, we tested the sensitivity of xKv1.4 channels to 4-AP and TEA. Kv channels were activated with 200-ms depolarizing pulses from −80 to +40 mV every 30 s. 4-AP blocked xKv1.4 channels with a K_d of 3.1±0.5 mM, whereas TEA up to 160 mM barely inhibited xKv1.4 channels. Quinidine is a non selective ion channel blocker, which blocks mammalian Kv1.4 with a K_d of <10 μM [38]. We found that externally applied quinidine blocked xKv1.4 with a K_d of 10 μM. Several Kv subfamilies show high affinity binding to peptide toxins, including charybdotoxin (CTX), margatoxin (MgTX), or dendrotoxin (DTX). The peptide toxins CTX, MgTX, or DTX did not affect the amplitude or inactivation of all

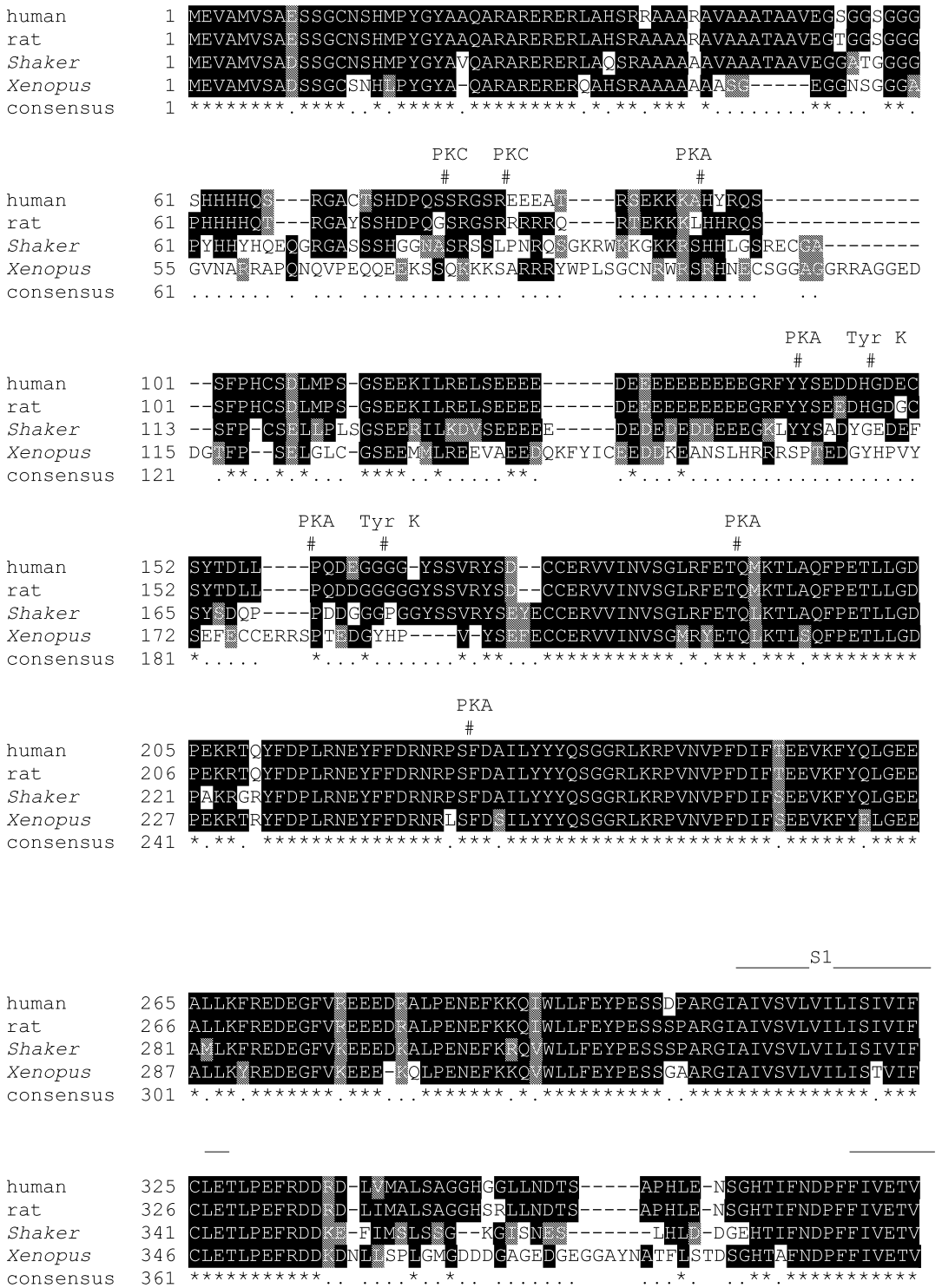

Fig. 2. Colinear alignment of the deduced amino acid sequence of Kv1.4 from human, rat, *Shaker*, and *X. laevis*. Amino acids are designated by the single letter code. Identity between xKv1.4 and the mammalian homologues is stressed by the black background. Gray background indicates conservative amino acid substitution. The putative transmembrane domains (S1–S6) are demarcated by bars above the sequence. Potential phosphorylation sites for PKA, PKC, and tyrosine kinase of xKv1.4 are indicated by #. Amino acid numbering is shown to the left of the sequence. Gaps, introduced to facilitate alignment and comparison between the proteins, are indicated by dashed lines. Sequences for human, mouse and rat Kv1.4 were obtained from GenBank/EMBL. Sequences were aligned using Multiple Sequence Alignment (European Bioinformatics Institute).

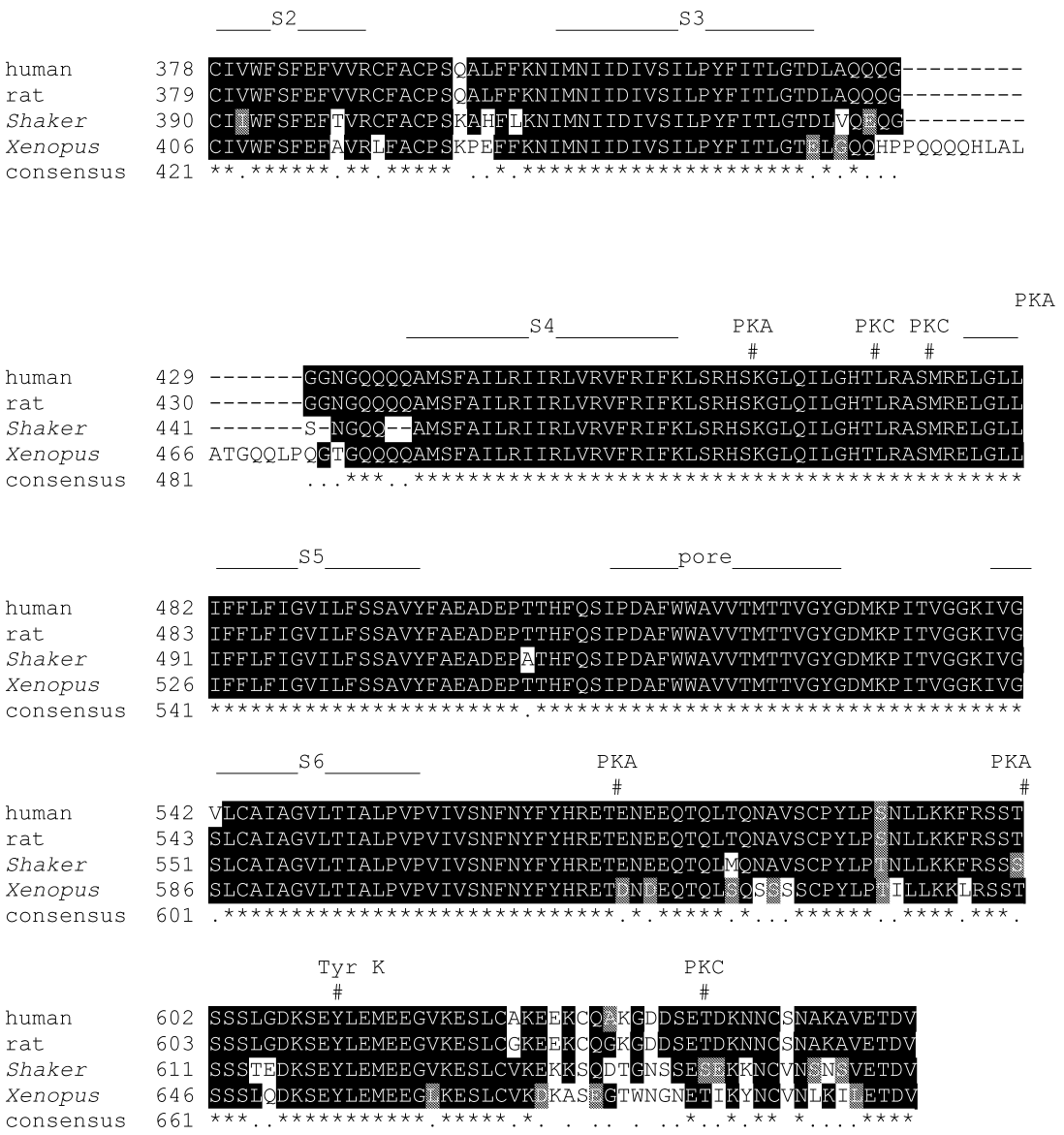

Fig. 2. (*continued*)

Table 1
Similarities (%) of the primary sequence among *Shaker*, *Xenopus* (xKv1.4), rat (rKv1.4), and human Kv1.4 (hKv1.4) channels

	Shaker	xKv1.4m	xKv1.4	rKv1.4	hKv1.4
xKv1.4	35	95	100	65	72
xKv1.4m	35	100	95	43	71

tested Kv1.4 currents. Thus, according to our data, xKv1.4 does not differ in its pharmacological profile from those described for mammalian Kv1.4 (Table 2).

Our experiments show that the biophysical and pharmacological signature of xKv1.4 corresponds to the A-current reported in *Xenopus* neurons. Furthermore, the biophysical

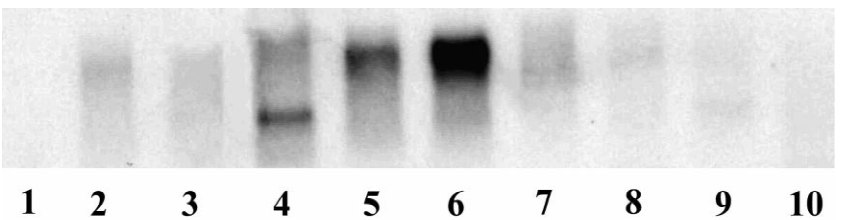

Fig. 3. Expression of xKv1.4 in adult *X. laevis*. RNAs were separated by electrophoresis on an agarose gel and transferred onto a nylon filter. Filter was incubated with a cDNA probe for xKv1.4. 1, ovary; 2, lung; 3, skin; 4, brain; 5, spleen; 6, muscle; 7, heart; 8, kidney; 9, intestine; 10, liver.

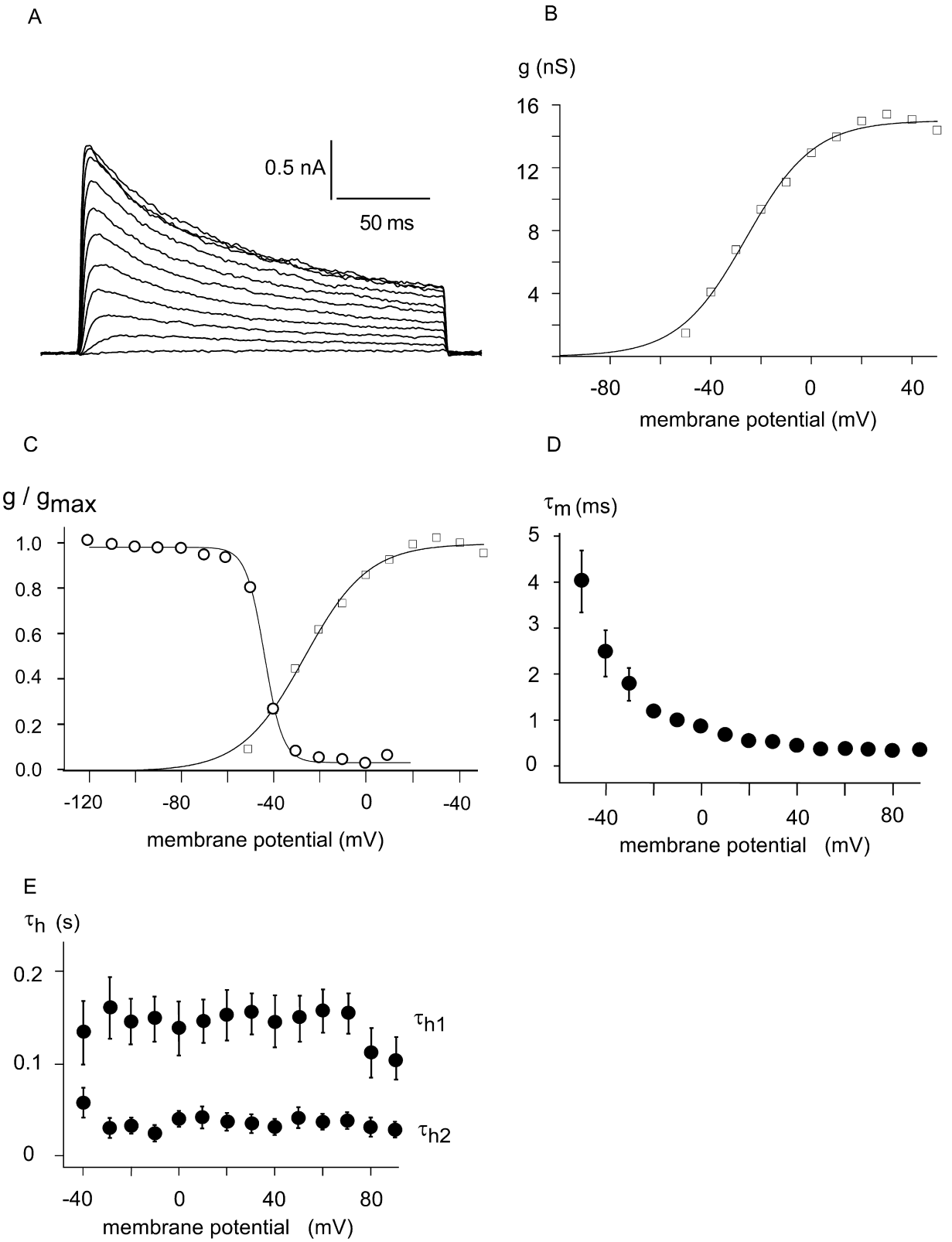

Fig. 4. K_v currents recorded from an RBL cell injected with Kv1.4 cRNA. The bath solution was normal external saline and the pipette solution contained a KF solution (see Material and methods). (A) Family of K_v currents recorded from an injected RBL cell. Membrane current responses to depolarizing voltage steps from −50 to +50 mV in 10-mV increments from a holding potential of −100 mV. The pulses were delivered every 30 s. Leak currents and capacitative currents were subtracted. (B) Peak conductance plotted against membrane potential of the K^+ current in (A) after leak subtraction. $V_n = -26$ mV, $k = 14$, and $g_{K_{max}} = 15$ nS. (C) Inactivation curve was obtained using a 1-s prepulse from −120 to +10 mV in 10-mV increments followed by a 30-ms test pulse to +40 mV. Data points represent the mean of five cells. Standard deviations are smaller than the size of the symbol. Data points were fit to a Boltzmann distribution. Mean half inactivation was −43 mV. (D) Voltage dependence of mean time constants of activation (five cells). (E) Voltage dependence of inactivation (five cells). τ_f is fast component of inactivation; τ_s is slow component of inactivation.

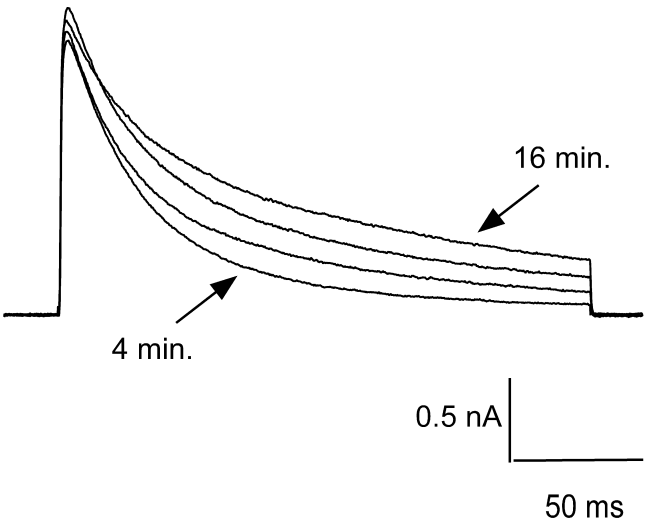

Fig. 5. Kinetics during different times after break-in. KF pipette solution was used for whole-cell recordings (six cells). Current responses of a representative cell at 4, 8, 12, and 16 min after break-in as indicated (arrows). A progressive decrease in inactivation was observed.

and pharmacological properties of xKv1.4 are indistinguishable from mammalian Kv1.4.

4. Discussion

Electrical activity orchestrates neuronal plasticity during development and learning [2,8,11,20,22]. Patch clamp experiments on *Xenopus* neurons and muscle cells have revealed several distinct types of ion channels, including Na^+-channels, Ca^{2+}-channels, and K^+-channels [12,24,35]. Recently, cloning and sequencing analysis provided evidence for voltage-gated K^+-channels in *Xenopus* neurons (xKv1.1, xKv1.2, xKv2.1, xKv2.2, and xKv3.1) [5,14,24,30,33,34]. Furthermore, electrophysiological evidence exists for an A-type current in *Xenopus* neurons and muscle fibers [12,30]. In the present study, we identified a *Shaker* channel, which is homologous to the mammalian Kv1.4. Our results demonstrate that the biophysical and pharmacological signature of xKv1.4 and hKv1.4 are comparable.

4.1. Comparison of voltage-gated K^+-channels in amphibians

Most voltage-dependent K^+-channels are encoded by genes related to *Shaker* (Kv1), *Shab* (Kv2), *Shaw* (Kv3), or *Shal* (Kv4), originally identified in *Drosophila* [6]. In *X. laevis*, K^+-currents encoded by xKv1.1 and xKv2.2 have been identified in primary spinal neurons [29,34]. Heterologous expression in *Xenopus* oocytes of ion channels encoded by Kv1.1 and Kv2.2 revealed voltage-dependent outward rectifying, delayed K^+-currents differing in their kinetic and pharmacological properties. K^+-channels encoded by Kv1.1 activated at potentials positive to -40 mV, showed a sustained current, and were sensitive to external TEA [29]. K^+-channels encoded by xKv2.2 showed a lower sensitivity to TEA [28].

The biophysical and pharmacological properties of the K^+-channel encoded by xKv1.4 described in this study resemble the A-type current reported in *Xenopus* primary spinal neurons [28]. These ion channels show a transient current, and are sensitive to 4-AP but not to TEA [28]. K^+-channels with transient current are encoded by different genes, including Kv1.4, Kv3.3, Kv3.4, Kv4.1, Kv4.2, and Kv4.3 or a combination of Kv1.x and Kvβ [6,26]. Kv3.3 and Kv3.4 are very sensitive to TEA (K_d 0.2 mM), whereas Kv4.1 and Kv4.2 are less sensitive to TEA ($K_d >$ 10 mM and 15 mM, respectively) [6]. According to this pharmacological property, A-current in *Xenopus* resembles more Kv1.4 than any other known K^+-channel. Thus, we conclude that the substrate for the A-current in *Xenopus* more closely resembles Kv1.4 than any other known K^+-channel.

4.2. Comparison of Kv1.4 isoforms

The main biophysical hallmarks of K^+-channels encoded by Kv1.4 are rapid activation and inactivation, frequency-dependent cumulative inactivation, and K^+ dependence of the ion current [25,36]. A-type K^+-channels show a C-type and an N-type inactivation. N-type inactivation in channels encoded by Kv1.4 is due to a 'ball and chain' mechanism [6], originally proposed for the inactivation of Na^+-channels [3]. The first 174 amino acids on the N-terminal region show significant divergences to other K^+-channels encoded by *Shaker*-like genes. These residues are the structural substrate for the 'ball' mechanism in K^+-channels encoded by Kv1.4. The similarity of the initial 174 amino acids between xKv1.4 and hKv1.4 is 31% and only 13% between xKv1.4 and hKv1.3. However, xKv1.4 shows a few segments with additional amino acids not present in mammalian Kv1.4, which contribute to a lower similarity. In contrast, comparison of the initial 25 amino acids in xKv1.4 with hKv1.4 showed 72% similarity. The structural similarities between xKv1.4 and mammalian Kv1.4 indicate that N-type inactivation in xKv1.4 is due to similar 'ball and chain' mechanism as in mammalian Kv1.4 [6].

Ion channels encoded by Kv1.4 show a strong K^+-dependence in their gating and kinetic properties [19,25]. Omission of extracellular K^+ reduces the current and increase in extracellular K^+ decreases inactivation and frequency-dependent cumulative inactivation [4,6,9,25]. We show a similar strong K^+-dependence of xKv1.4. Decreasing inactivation and reducing frequency-dependent cumulative inactivation in elevated $[K^+]_e$, are attributed to electrostatic repulsion between the inactivation gate and K^+ and, thus, accelerates the exit of the inactivation gate from the pore [6,16]. The initial 25 amino acids of xKv 1.4

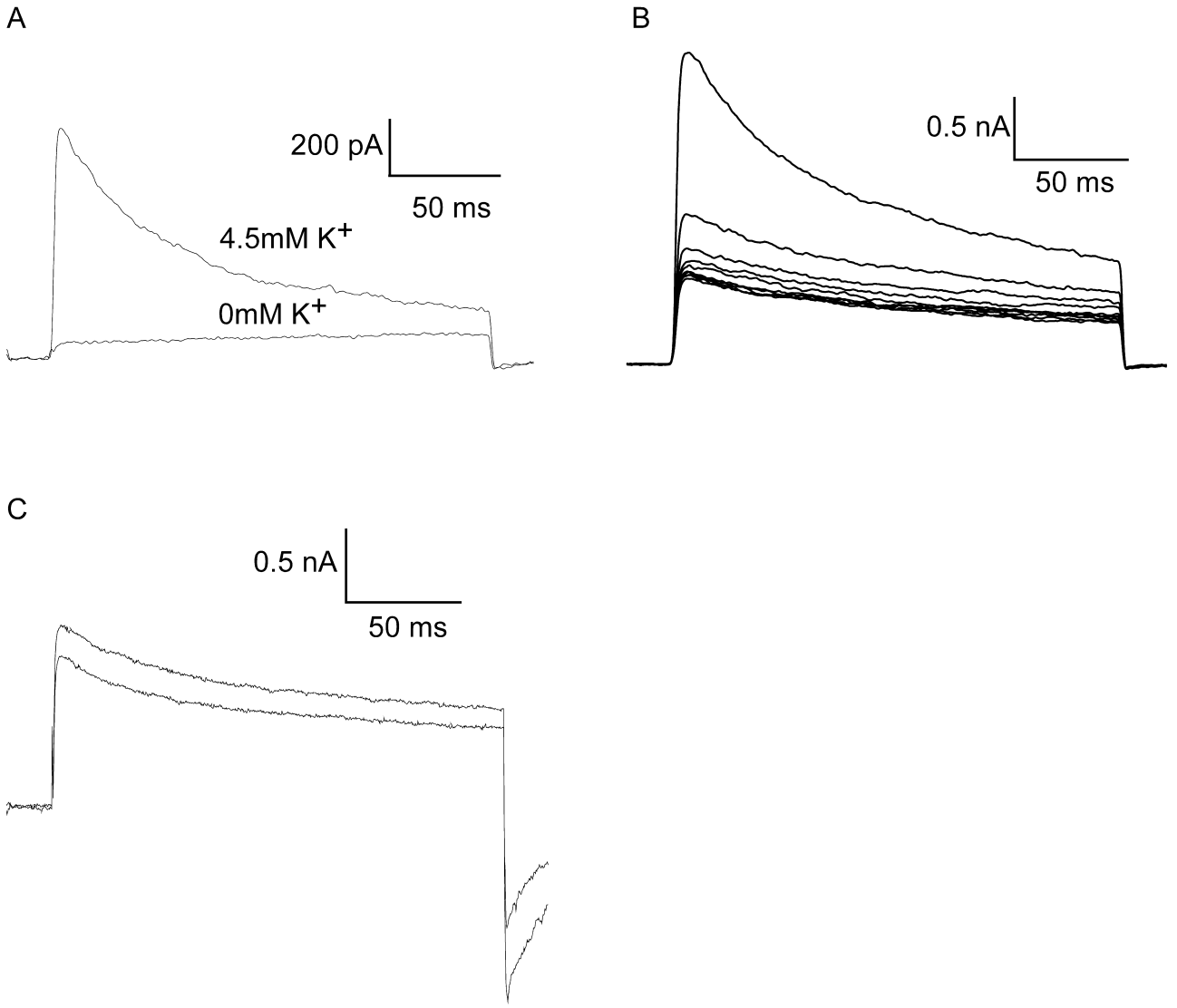

Fig. 6. $[K^+]_e$ dependence of xKv1.4. The pipette solution was KF. (A) Current responses to depolarizing voltage steps to +40 mV from a holding potential of −80 mV in normal mammalian bath solution (4.5 mM K^+) and K^+-free mammalian bath solution. In normal mammalian bath solution, the cell reveals a rapidly activating and inactivating current. After superfusion of the cell with K^+-free bath solution, the current is largely diminished. (B) Frequency-dependent cumulative inactivation of a cell bathed in normal mammalian bath solution. Currents were elicited by depolarizing voltage steps to +40 mV from a holding potential of −80 mV and were collected every second. The current during the second and the following voltage pulses was significantly inactivated. Current responses to 10 voltage pulses are shown. (C) Frequency-dependent cumulative inactivation of a cell bathed in a high K^+ solution (160 mM K^+). Currents were elicited by depolarizing voltage steps every second. Extent of frequency-dependent cumulative inactivation is significantly smaller compared to normal mammalian bath solution. Current responses to the first and tenth voltage step are shown.

are almost identical to hKv1.4 and, furthermore, xKv1.4 contains lysine at the outer vestibule. Nitrogen-containing amino acid residues in the outer pore region contribute significantly to the K^+-dependence of K^+-channels [19]. Therefore, structural similarities correlate with biophysical similarities of Kv1.4 channels.

In conclusion, our study suggests that the biophysical similarities of xKv1.4 and mammalian Kv1.4 are due to conserved structures in particular regions of xKv1.4 and mammalian Kv1.4.

4.3. Possible physiological significance of Kv1.4 in the amphibian nervous system

We identified xKv1.4 expression in the brain, muscle and spleen. Gating and kinetic properties of K^+-channels orchestrate neuronal excitability by setting resting membrane potential and by determining latency, duration, and firing pattern of action potentials [17]. A-currents mainly affect latency, duration, and repetitive firing properties of neurons. Electrophysiological detection of an A-current in

Table 2
Pharmacology of xKv1.4 and rKv1.4

	4-AP (mM)	Quinidine (μM)	TEA (mM)	CTX (nM)	MgTx (nM)	DTX (nM)
xKv1.4	3	10	>160	>50	>100	>100
rKv1.4	1.3[a]	<10[b]	>100[a]	>40[a]	n.d.	>200[a]

Numbers are mean±S.D. of K_d values and have been determined by fitting $I_K = I_{K,con}\{1+(K_d/[X])\}$ to dose–response curve, assuming that a single drug molecule binds to one K^+ channel. n.d., not determined; '>' no effect up to the concentration indicated; '<' K_d smaller than the concentration indicated; between five and eight cells have been studied to estimate K_d.
[a] Chandy and Gutman [6].
[b] Yang et al. [38].

Xenopus primary spinal neurons correlates with shortening of the duration of action potentials and a burst of action potentials as a response to maintained depolarization instead of a continuous firing [30]. According to our experiments, the A-current in *Xenopus* primary spinal neurons or muscle cells seems to be encoded by xKv1.4. In line with our arguments, a xKv1.4m has been cloned and sequenced from *Xenopus* muscle [13]. Since xKv1.4 rapidly activates following a depolarization, it could significantly contribute to shortening of the duration of action potentials. Maintained depolarization inactivates Kv1.4 channels and, thus, may not be important for the phasic property, however, the inactivation of Kv1.4 may lead to lengthening of action potentials and facilitation of synaptic transmission [10]. Therefore, another ion channel could be responsible for the refractoriness. Sympathetic neurons of adult rats respond either tonically or phasically to a maintained depolarizing stimulus. In these neurons, the slowly activating M-current determines the phasic property [37]. M-currents have been detected electrophysiologically in bullfrog sympathetic neurons [1], and, thus, could contribute to the intrinsic electrophysiological properties of amphibian neurons.

Acknowledgements

The authors would like to thank Katharina Ruff for excellent technical support. This work was supported by grants from the FWF (13395) and the University of Salzburg to HHK and DFG (Gr848/4-1 and Gr848/4-2) to SG.

References

[1] P.R. Adams, D.A. Brown, A. Constanti, M-currents and other potassium currents in bullfrog sympathetic neurones, J. Physiol. 330 (1982) 537–572.
[2] D.L. Alkon, T.J. Nelson, W. Zhao, S. Cavallaro, Time domains of neuronal Ca^{2+} signaling and associative memory: steps through a calexcitin, ryanodine receptor, K^+ channel cascade, Trends Neurosci. 21 (1998) 529–537.
[3] C.M. Armstrong, F. Bezanilla, Inactivation of the sodium channel. II. Gating current experiments, J. Gen. Physiol. 70 (1977) 567–590.
[4] T. Baukrowitz, G. Yellen, Modulation of K^+ current by frequency and external $[K^+]$: a tale of two inactivation mechanisms, Neuron 15 (1995) 951–960.
[5] C. Burger, A.B. Ribera, *Xenopus* spinal neurons express Kv2 potassium channel transcripts during embryonic development, J. Neurosci. 16 (1996) 1412–1421.
[6] K.G. Chandy, G.A. Gutman, Voltage-gated K^+ channel genes, in: R.A. North (Ed.), CRC Handbook of Receptors and Channels, CRC Press, Boca Raton, FL, 1994, pp. 1–71.
[7] P. Chomczynski, N. Sacchi, Single-step method of RNA isolation by acid guanidinium thiocyanate–phenol–chloroform extraction, Anal. Biochem. 162 (1987) 156–159.
[8] E.C. Cooper, A. Milroy, Y.N. Jan, L.Y. Jan, D.H. Lowenstein, Presynaptic localization of Kv1.4-containing A-type potassium channels near excitatory synapses in the hippocampus, J. Neurosci. 18 (1998) 965–974.
[9] C. Eder, R. Klee, U. Heinemann, Modulation of A-currents by $[K^+]_o$ in acutely isolated pyramidal neurones of juvenile rat entorhinal cortex and hippocampus, Neuroreport 7 (1996) 1565–1568.
[10] J. Engel, J. Rabba, D. Schild, A transient, RCK4-like K^+ current in cultured *Xenopus* olfactory bulb neurons, Pflügers Arch. 432 (1996) 845–852.
[11] J.E. Engel, C.F. Wu, Genetic dissection of functional contributions of specific potassium channel subunits in habituation of an escape circuit in *Drosophila*, J. Neurosci. 18 (1998) 2254–2267.
[12] U. Ernsberger, N.C. Spitzer, Convertible modes of inactivation of potassium channels in *Xenopus* myocytes differentiating in vitro, J. Physiol. 484 (1995) 313–329.
[13] M. Fry, G. Paterno, F. Moody-Corbett, Cloning and expression of three K^+ channel cDNAs from *Xenopus* muscle, Brain Res. Mol. Brain Res. 90 (2001) 135–148.
[14] D. Gurantz, N.J. Lautermilch, S.D. Watt, N.C. Spitzer, Sustained upregulation in embryonic spinal neurons of a Kv3.1 potassium channel gene encoding a delayed rectifier current, J. Neurobiol. 42 (2000) 347–356.
[15] O.P. Hamill, A. Marty, E. Neher, B. Sakmann, F.J. Sigworth, Improved patch-clamp techniques for high-resolution current recording from cells and cell-free membrane patches, Pflügers Arch. 391 (1981) 85–100.
[16] R.E. Harris, H.P. Larsson, E.Y. Isacoff, A permanent ion binding site located between two gates of the Shaker K^+ channel, Biophys. J. 74 (1998) 1808–1820.
[17] B. Hille, Ionic Channels in Excitable Membranes, 2nd Edition, Sinauer Associates, MA, 1992.
[18] S.R. Ikeda, F. Soler, R.D. Zühlke, R.H. Joho, D.L. Lewis, Heterologous expression of the human potassium channel Kv2.1 in clonal mammalian cells by direct cytoplasmic microinjection of cRNA, Pflügers Arch. 422 (1992) 201–203.
[19] H. Jäger, H. Rauer, A.N. Nguyen, J. Aiyar, K.G. Chandy, S. Grissmer, Regulation of mammalian *Shaker*-related K^+ channels: evidence for non-conducting closed and non-conducting inactivated states, J. Physiol. 506 (1998) 291–301.
[20] K. Kandler, L.C. Katz, Coordination of neuronal activity in developing visual cortex by gap junction-mediated biochemical communication, J. Neurosci. 18 (1998) 1419–1427.
[21] M.A. McCloskey, M.D. Cahalan, G protein control of potassium channel activity in a mast cell line, J. Gen. Physiol. 95 (1990) 205–227.
[22] M.D. Neely, J.G. Nicholls, Electrical activity, growth cone motility and the cytoskeleton, J. Exp. Biol. 198 (1995) 1433–1446.

[23] N.A. Nguyen, J.C. Kath, D.C. Hanson, M.S. Biggers, P.C. Canniff, C.B. Donovan, R.J. Mather, M.J. Bruns, H. Rauer, J. Aiyar, A. Lepple-Wienhues, G.A. Gutman, S. Grissmer, M.D. Cahalan, K.G. Chandy, Novel nonpeptide agents potently block the C-type inactivated conformation of Kv1.3 and suppress T cell activation, Mol. Pharmacol. 50 (1996) 1672–1679.

[24] D.K. O'Dowd, A.B. Ribera, N.C. Spitzer, Development of voltage-dependent calcium, sodium, and potassium currents in *Xenopus* spinal neurons, J. Neurosci. 8 (1988) 792–805.

[25] L.A. Pardo, S.H. Heinemann, H. Terlau, U. Ludewig, C. Lorra, O. Pongs, W. Stühmer, Extracellular K^+ specifically modulates a rat brain K^+ channel, Proc. Natl. Acad. Sci. USA 89 (1992) 2466–2470.

[26] O. Pongs, T. Leicher, M. Berger, J. Roeper, R. Bahring, D. Wray, K.P. Giese, A.J. Silva, J.F. Storm, Functional and molecular aspects of voltage-gated K channel beta subunits, Ann. NY Acad. Sci. 868 (1999) 344–355.

[27] H. Rauer, S. Grissmer, Evidence for an internal phenylalkylamine action on the voltage-gated potassium channel Kv1.3, Mol. Pharmacol. 50 (1996) 1625–1634.

[28] A.B. Ribera, A potassium channel gene is expressed at neural induction, Neuron 5 (1990) 691–701.

[29] A.B. Ribera, D.A. Nguyen, Primary sensory neurons express a *Shaker*-like potassium channel gene, J. Neurosci. 13 (1993) 4988–4996.

[30] A.B. Ribera, N.C. Spitzer, Differentiation of IKA in amphibian spinal neurons, J. Neurosci. 10 (1990) 1886–1891.

[31] J. Roeper, C. Lorra, O. Pongs, Frequency-dependent inactivation of mammalian A-type K^+ channel Kv1.4 regulated by Ca^{2+}/calmodulin-dependent protein kinase, J. Neurosci. 17 (1997) 3379–3391.

[32] F. Sanger, S. Nicklen, A.R. Coulsen, DNA sequencing with chain-terminating inhibitors, Proc. Natl. Acad. Sci. USA 74 (1977) 5463–5467.

[33] N.C. Spitzer, J.E. Lamborghini, The development of the action potential mechanism of amphibian neurons isolated in culture, Proc. Natl. Acad. Sci. USA 73 (1976) 1641–1645.

[34] N.C. Spitzer, A.B. Ribera, Development of electrical excitability in embryonic neurons: mechanisms and roles, J. Neurobiol. 37 (1998) 190–197.

[35] A.E. Spruce, W.J. Moody, Developmental sequence of expression of voltage-dependent currents in embryonic *Xenopus laevis* myocytes, Dev. Biol. 154 (1992) 11–22.

[36] W. Stühmer, J.P. Ruppersberg, K.H. Schröter, B. Sakmann, M. Stocker, K.P. Giese, A. Perschke, A. Baumann, O. Pongs, Molecular basis of functional diversity of voltage-gated potassium channels in mammalian brain, EMBO J. 8 (1989) 3235–3244.

[37] H.S. Wang, D. McKinnon, Potassium currents in rat prevertebral and paravertebral sympathetic neurones: control of firing properties, J. Physiol. 485 (1995) 319–335.

[38] T. Yang, D.J. Snyders, D.M. Roden, Inhibition of cardiac potassium currents by the vesnarinone analog OPC-18790: comparison with quinidine and dofetilide, J. Pharmacol. Exp. Ther. 280 (1997) 1170–1175.